Molecular Therapy
Nucleic Acids
Original Article

lncNBAT1/APOBEC3A is a mediator of HBX-induced chemoresistance in diffuse large B cell lymphoma cells

Jianguo Li,[1,4] Yaqi Chen,[1,4] Xuecong Guo,[1] Xiaofei Bai,[1] Xu Xu,[2] Tong Han,[1] Ailing Tan,[1] Nana Liu,[1] Yuchen Xia,[1] Qiaoyi Sun,[1] Xudong Guo,[1,3] Jie Chen,[2] and Jiuhong Kang[1]

[1]Clinical and Translational Research Center of Shanghai First Maternity and Infant Hospital, Shanghai Key Laboratory of Maternal Fetal Medicine, Shanghai Key Laboratory of Signaling and Disease Research, Frontier Science Center for Stem Cell Research, National Stem Cell Translational Resource Center, School of Life Sciences and Technology, Tongji University, Shanghai 200092, China; [2]Department of Hematology, Changhai Hospital, Second Military Medical University, Shanghai 200433, China; [3]Institute for Advanced Study, Tongji University, Shanghai 200092, China

Individuals with diffuse large B cell lymphoma (DLBCL) infected with hepatitis B virus (HBV) have worse chemotherapy efficacy and poorer outcomes. It is still unclear whether long noncoding RNAs (lncRNAs) serve as prognostic and therapeutic targets in the chemotherapy resistance of individuals with DLBCL and HBV infection. Here we found that the core component of HBV (HBX) directly upregulated the expression of lncNBAT1, which was closely associated with the chemotherapy outcomes of HBV-infected individuals with DLBCL. Upregulation of lncNBAT1 reduced the sensitivity of DLBCL cells to chemotherapeutic agents (methotrexate [MTX] or cytarabine [Ara-C]) that induced S phase arrest, whereas knockdown of lncNBAT1 significantly relieved the chemoresistance of HBX-expressing DLBCLs. Mechanistically, lncNBAT1 could interact with the signal transducer and activator of transcription 1 (STAT1) to prevent its enrichment at the promoter region of the functional target gene apolipoprotein B mRNA editing enzyme catalytic subunit 3A (APOBEC3A), inhibiting expression of APOBEC3A and inducing resistance to MTX in DLBCL cells. Furthermore, clinical data analysis showed that lncNBAT1 and APOBEC3A expression was closely related to the poor prognosis and short survival of individuals with DLBCL. Our findings suggest a potential prognostic marker and a candidate lncRNA target for treating HBV-infected individuals with DLBCL.

INTRODUCTION

Diffuse large B cell lymphoma (DLBCL) is the most common heterogeneous lymphoid malignancy, accounting for approximately 30%–40% of non-Hodgkin's lymphomas.[1] More than half of individuals with DLBCL can be cured by chemotherapy, radiotherapy combined with immunotherapy, or autologous stem cell transplantation.[2] However, approximately 30%–40% of individuals will develop relapsed or refractory disease.[3] Chemoresistance, as a multifactorial phenomenon, is an important factor in individuals with relapsed or refractory DLBCL.[3–5] Accumulating evidence suggests that hepatitis B virus (HBV) infection is a major obstacle for treatment of DLBCL.[6–8] Epidemiologic investigations in HBV endemic areas show that HBV infection is more common in individuals with non-Hodgkin`s lymphoma (NHL) than in the general population (19.94% versus 7.18%).[9–12] Additionally, epidemiological and clinical studies suggest that the chemotherapy efficiency of HBV-infected individuals with DLBCL is significantly lower than that of individuals with DLBCL without HBV infection, eventually causing a poor prognosis.[7] Therefore, the present clinical treatments for HBV-infected individuals with DLBCL cannot effectively improve the prognosis, and it is necessary to clarify the mechanism of HBV infection-induced chemotherapy resistance and develop new strategies for the treatment of HBV-infected individuals with DLBCL.

At present, an estimated 400 million people are living with chronic HBV infection, which leads to nearly 1 million deaths annually.[13–15] HBV infection is a major risk factor for and is associated with 80% of hepatocarcinogenesis.[16] The core component of HBV (HBX) is critical for the self-renewal, tumorigenicity, and drug resistance of

Received 7 May 2021; accepted 21 January 2022;
https://doi.org/10.1016/j.omtn.2022.01.015.

[4]These authors contributed equally

Correspondence: Xudong Guo, Clinical and Translational Research Center of Shanghai First Maternity and Infant Hospital, Shanghai Key Laboratory of Maternal Fetal Medicine, Shanghai Key Laboratory of Signaling and Disease Research, Frontier Science Center for Stem Cell Research, National Stem Cell Translational Resource Center, School of Life Sciences and Technology, Tongji University, Shanghai 200092, China
E-mail: 19504@tongji.edu.cn
Correspondence: Jie Chen, Department of Hematology, Changhai Hospital, Second Military Medical University, Shanghai 200433, China
E-mail: chenjiedoctor@163.com
Correspondence: Jiuhong Kang, Clinical and Translational Research Center of Shanghai First Maternity and Infant Hospital, Shanghai Key Laboratory of Maternal Fetal Medicine, Shanghai Key Laboratory of Signaling and Disease Research, Frontier Science Center for Stem Cell Research, National Stem Cell Translational Resource Center, School of Life Sciences and Technology, Tongji University, Shanghai 200092, China
E-mail: jhkang@tongji.edu.cn

hepatocellular carcinoma (HCC).[17] Integration of large HBV DNA segments and expression of HBX protein can also be detected in the lymphoma tissue of individuals with DLBCL.[18–20] Ren et al.[21] performed a comprehensive genetic study of HBV-infected individuals with DLBCL and found that HBV infection might affect p53 signaling, Forkhead box O (FOXO) signaling, and immune evasion to promote survival and growth of HBV-infected DLBCL cells. Our previous study also found that HBX protein specifically blocked activation of checkpoint kinase 2 (CHK2), reducing sensitivity to chemotherapeutic agents in DLBCL cells.[22] Thus, HBV infection is closely related to development and prognosis of individuals with DLBCL receiving chemotherapy, but research regarding the mechanisms and therapeutic targets of HBV affecting tumorigenesis and chemotherapy outcomes of DLBCL is still limited.

Long noncoding RNAs (lncRNAs), defined as transcripts of longer than 200 nt without coding potential,[23] have been reported to mediate critical processes of tumorigenesis, invasion, metastasis, and chemoresistance.[24] The lncRNA PDIA3P1 is closely related to survival of individuals with HCC and reduces the chemotherapy sensitivity of doxorubicin by binding with miR-125a/b and miR-214 in HCC cells.[25] Associated with the progression and poor outcome of small cell lung cancer, the lncRNA TUG1 mediates resistance to cisplatin and etoposide.[26] A study directed at DLBCL identified a large number of lncRNAs that are differentially expressed compared with normal B cells, indicating that lncRNAs may play critical roles in DLBCL development.[27] A previous study found that the lncRNA DBH-AS1 regulates FN1 mRNA stability by binding BUD13 and promoting proliferation, migration, and invasion of DLBCL cells.[28] It was also found that HBV infection can lead to aberrant expression of lncRNAs, but the role of lncRNAs in the poor chemotherapy outcomes of individuals with DLBCL and HBV infection is still unclear.

Here we found that lncNBAT1, upregulated by HBX, was closely related to the progression and survival of individuals with DLBCL. Targeting lncNBAT1 rescued the resistance of S phase arrest-inducing chemotherapeutic agents (methotrexate [MTX] or cytarabine [Ara-C]) caused by HBX overexpression. Mechanistically, lncNBAT1 decreased APOBEC3A expression by reducing STAT1 enrichment at the *APOBEC3A* gene promoter, and APOBEC3A was the key target linking lncNBAT1 to the resistance of chemotherapy drugs.

RESULTS

HBX upregulates expression of lncNBAT1, leading to chemoresistance to S phase arrest chemotherapy in DLBCL

Our previous study found that HBV infection in individuals with DLBCL is closely correlated with poor chemotherapy outcomes.[9,22] To obtain chemoresistance-related lncRNAs, we analyzed the microarray data from four chemotherapy-sensitive and three chemotherapy-resistant DLBCL tissue samples after treatment with first-line chemotherapeutic agents, including MTX and Ara-C (GSE23501) (Figure 1A). Among the top 10 differentially expressed lncRNAs, we found that only expression of lncNBAT1 (chromosome 6: 22, 133, 205-22, 147, 193), but not the other 9 differentially expressed lncRNAs, was negatively correlated with the survival of individuals with DLBCL (Figures 1B, 1C, and S1). To elucidate the possible biological pathways by which lncNBAT1 is involved in DLBCL pathogenesis, we performed a gene set enrichment analysis (GSEA) using the transcriptome data of DLBCL (GSE56315). The GSEA showed that the gene signatures of response to drug and positive regulation of cell cycle arrest were enriched in individuals with low expression of lncNBAT1 (Figure 1D). These data suggest that lncNBAT1 might be involved in the cancer drug response and regulation of cell cycle arrest. Moreover, lncNBAT1 was significantly upregulated by HBX overexpression (Figure 1E). Thus, we speculated that lncNBAT1 might be a key lncRNA molecule that mediates the HBX overexpression-induced resistance to MTX or Ara-C in DLBCL cells. We then focused on the relationship of HBX and lncNBAT1 and constructed a luciferase reporter of the *lncNBAT1* promoter. As shown in Figure 1F, HBX significantly enhanced the promoter activity of the *lncNBAT1* gene. To further clarify the exact binding sites responsible for the HBX-induced transcriptional activation of lncNBAT1, a chromatin immunoprecipitation (ChIP) assay was conducted, and we found that HBX could directly bind at −1,000 to 0 bp of the *lncNBAT1* gene promoter in SUDHL-4 cells (Figure 1G). These results demonstrated that HBX overexpression directly upregulated lncNBAT1 expression in SUDHL-4 cells. HBX overexpression could reduce the sensitivity to the chemotherapeutic drugs MTX and Ara-C, which are characterized by inducing S phase arrest.[22] To dissect the effect of lncNBAT1 on the chemosensitivity of DLBCL, we overexpressed lncNBAT1 in SUDHL-4 cells by using lentiviral transfection; the efficiency of lncNBAT1 overexpression is shown in Figure S2A. Then we tested the growth inhibition rate of control and lncNBAT1-expressing cells treated with MTX and Ara-C at half maximal inhibitory concentration (IC_{50}) values at 24, 48, and 72 h through cell counting and Cell Counting Kit 8 (CCK-8) assays. Compared with control cells, lncNBAT1 overexpression showed enhanced resistance to MTX and Ara-C after treatment for 48 and 72 h (Figures 1H, 1I, S2B, and S2C). We also confirmed that lncNBAT1 overexpression decreased the growth inhibition of SUDHL-4 cells under MTX and Ara-C treatment at different concentrations (Figures 1J and S2D). Cell cycle distribution analysis showed that lncNBAT1 overexpression significantly attenuated S phase arrest in SUDHL-4 cells upon treatment with MTX or Ara-C (Figures 1K and S2E). These findings indicated that lncNBAT1, directly upregulated by HBX, reduced the chemosensitivity of S phase arrest chemotherapeutic agents.

lncNBAT1 acts as a potent target in HBX-induced resistance to S phase arrest chemotherapy

Because overexpression of lncNBAT1 could result in enhanced chemoresistance upon MTX treatment, we tried to reverse the decreased chemosensitivity of HBX-expressing cells by reducing lncNBAT1. The expression of lncNBAT1 `was knocked down in HBX-expressing cells (Figure 2A), and our results showed that knockdown of lncNBAT1 significantly reversed the attenuation of HBX on proliferation inhibition and S phase arrest upon MTX treatment (Figures 2B–2D). To further assess the role of lncNBAT1 in HBX-induced

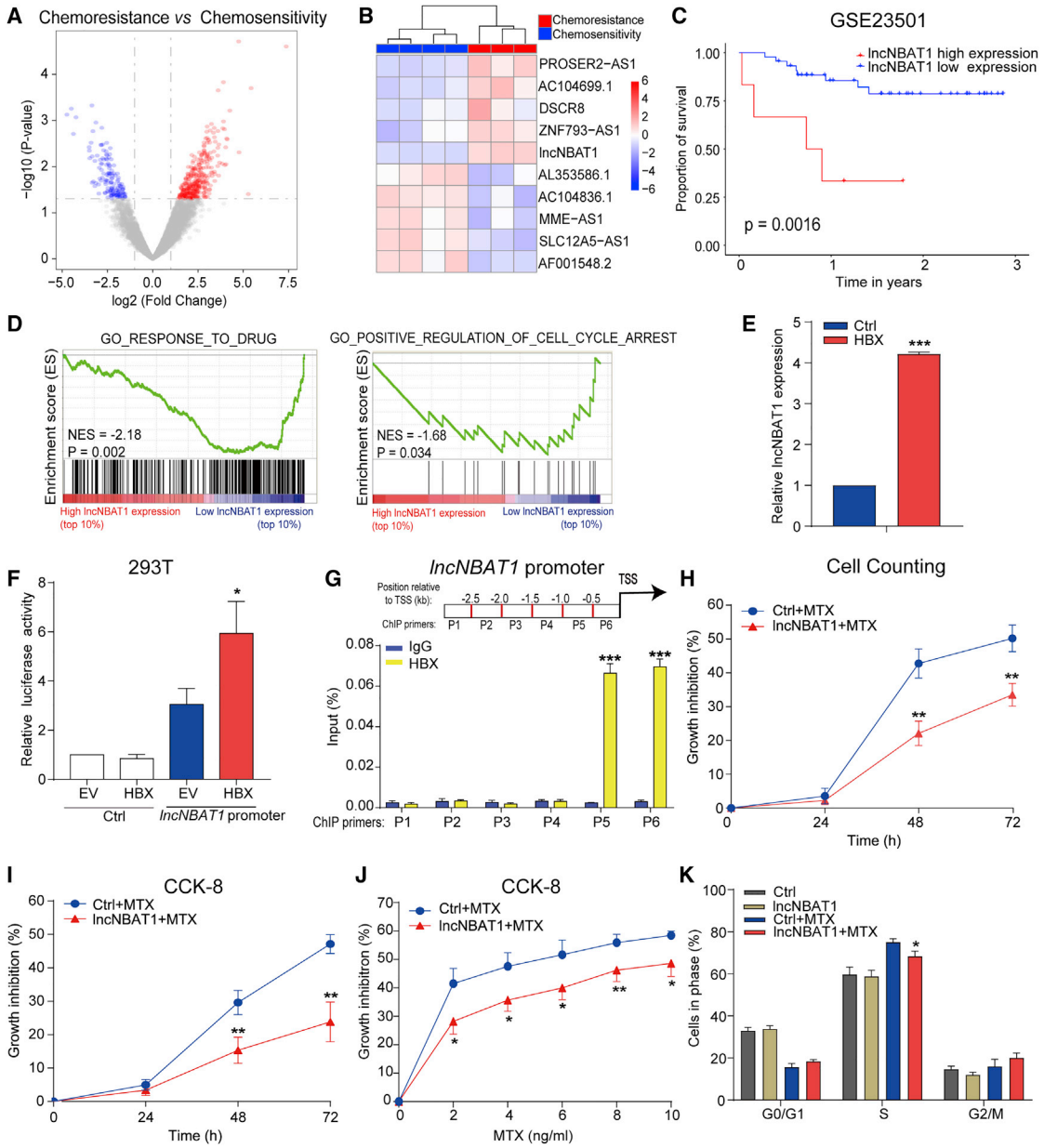

Figure 1. HBX upregulates expression of lncNBAT1, leading to chemoresistance to S phase arrest chemotherapy in DLBCL

(A) Volcano plot showing the differentially expressed lncRNAs in four chemotherapy-sensitive and three chemotherapy-resistant DLBCL tissue samples. (B) The top 10 dysregulated lncRNAs are shown in a heatmap for four chemotherapy-sensitive and three chemotherapy-resistant DLBCL tissue samples. (C) Survival was analyzed and compared between individuals with high and low lncNBAT1 expression using the Kaplan-Meier method. (D) GSEA results were plotted to visualize the correlation between expression of lncNBAT1 and genes related to the response to drug (left) or positive regulation of cell cycle arrest (right). (E) qRT-PCR analysis of the expression of lncNBAT1 in HBX-expressing SUDHL-4 cells compared with control cells. (F) Relative luciferase activity was detected after transient cotransfection of the HBX and *lncNBAT1* promoter in HEK293T cells. (G) Enrichment analysis of HBX protein at the *lncNBAT1* promoter in HBX-expressing SUDHL-4 cells. (H and I) Cell counting (H) and CCK-8 (I) analyses revealed the effect of lncNBAT1-overexpressing SUDHL-4 cells after MTX treatment (4.5 ng/mL) for 24, 48, and 72 h. (J) CCK-8 assay analysis showed the effect of lncNBAT1-overexpressing SUDHL-4 cells after MTX treatment at the indicated concentrations (2, 4, 6, 8, and 10 ng/mL) for 48 h. (K) Flow cytometry analysis showing the effect of lncNBAT1-overexpressing SUDHL-4 cells with or without MTX treatment (4.5 ng/mL) at 48 h. ** represents the significance of lncNBAT1 + MTX versus control (Ctrl) + MTX. The results were determined in triplicate, and the error bars represent the mean ± SD. *$p < 0.05$, **$p < 0.01$, and ***$p < 0.001$.

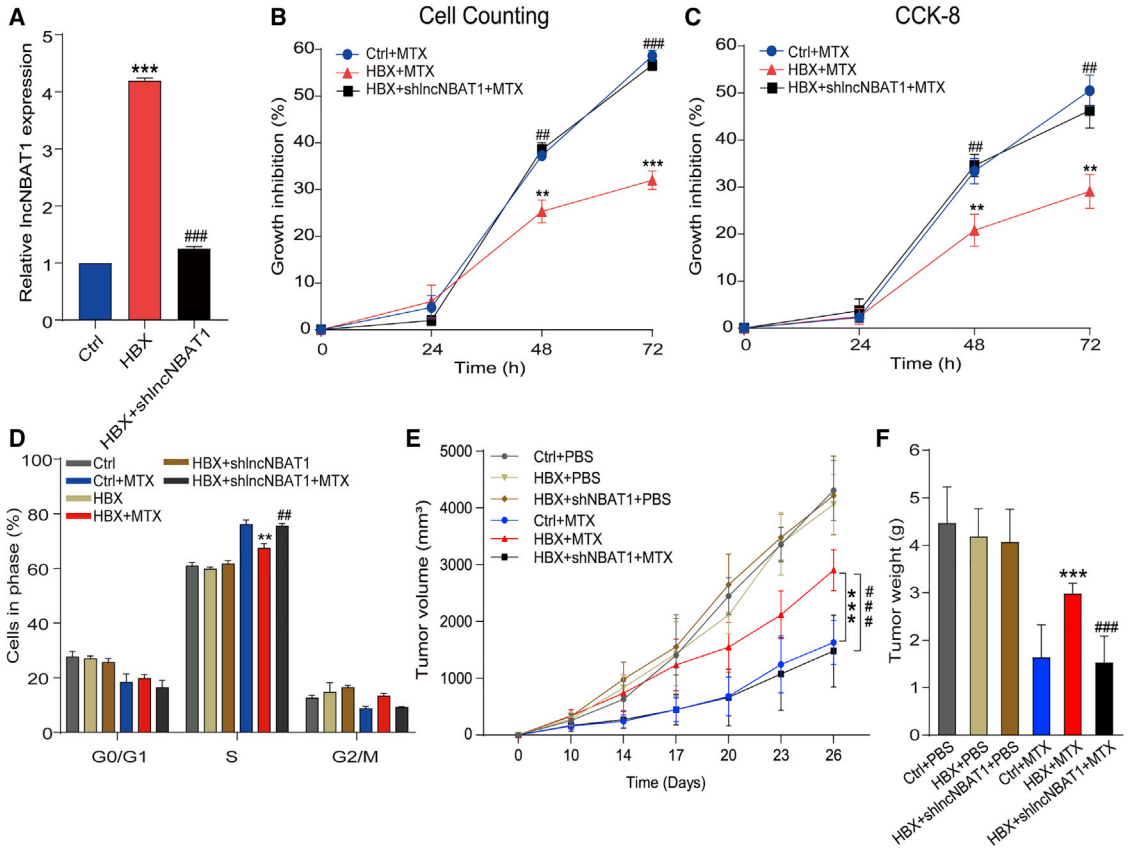

Figure 2. lncNBAT1 acts as a potential target in HBX-induced chemoresistance to S phase arrest chemotherapeutic agents

(A) qRT-PCR analysis of the expression of lncNBAT1 in Ctrl cells, HBX-overexpressing cells, and HBX-overexpressing cells with shlncNBAT1. (B–D) Cell counting (B), CCK-8 (C), and flow cytometry (D) analyses revealed the effect of lncNBAT1 knockdown in HBX-expressing cells after MTX treatment. * represents the significance of HBX versus Ctrl. # represents the significance of HBX + shlncNBAT1 versus HBX. (E and F) Tumor volumes (E) were measured every 3 days after day 14 after injection in the indicated groups (n = 9 per group). Tumor weight (F) was examined in nude mice for one of the batches on day 26 after injection. * represents the significance of HBX versus Ctrl. # represents the significance of HBX + shlncNBAT1 versus HBX. The results were determined in triplicate, and the error bars represent the mean ± SD. */#p < 0.05, **/##p < 0.01, ###p < 0.001.

chemoresistance, we administered HBX-expressing cells and HBX-expressing cells with shlncNBAT1 to non-obese diabetic (NOD)-severe combined immunodeficiency (SCID) mice. Two weeks after the injection, the mice were treated with MTX (10 mg/kg by intraperitoneal injection every 3 days), and the tumor sizes were measured (Figure S3A). Our results showed that the tumor volume and weight in mice injected with HBX-expressing SUDHL-4 cells were not reduced as effectively as in control mice injected with SUDHL-4 cells after MTX treatment, whereas knockdown of lncNBAT1 in HBX-expressing SUDHL-4 cells restored the suppressive effect of MTX on tumor volume and weight (Figures 2E and 2F). These results demonstrated that lncNBAT1 mediated HBX overexpression-induced resistance in DLBCL *in vitro* and *in vivo*.

The HBX/lncNBAT1 axis suppresses expression of APOBEC3A *in vitro* and *in vivo*

To investigate the downstream targets regulated by the HBX/lncNBAT1 axis, we tested the expression of differentially expressed genes between chemotherapy-sensitive and chemotherapy-resistant individuals with DLBCL in HBX-expressing cells. We found that HBX overexpression significantly downregulated expression of APOBEC3A, KLRB1, TNS4, and NMU and upregulated expression of MTCL1 (Figure 3A). Through gene expression profiling interactive analysis (http://gepia.cancer-pku.cn/), we found that only the APOBEC3A gene was expressed at significantly lower levels in DLBCL tumors (n = 47) than in non-tumors (n = 377) (Figures 3B and S4). Moreover, we found that expression of APOBEC3A was reduced in HBV-infected DLBCL tissue compared with normal tissue, suggesting that APOBEC3A might be a key target gene of HBX/lncNBAT1 (Figure 3C). Furthermore, knockdown of APOBEC3A also reduced proliferation inhibition and S phase arrest upon MTX treatment in SUDHL-4 cells (Figures 3D–3F). Next, we found that the mRNA and protein expression levels of APOBEC3A were decreased by overexpressing HBX, whereas knockdown of lncNBAT1 in HBX-overexpressing SUDHL-4 cells significantly restored expression of APOBEC3A (Figures 3G and 3H). HBX repressed expression of

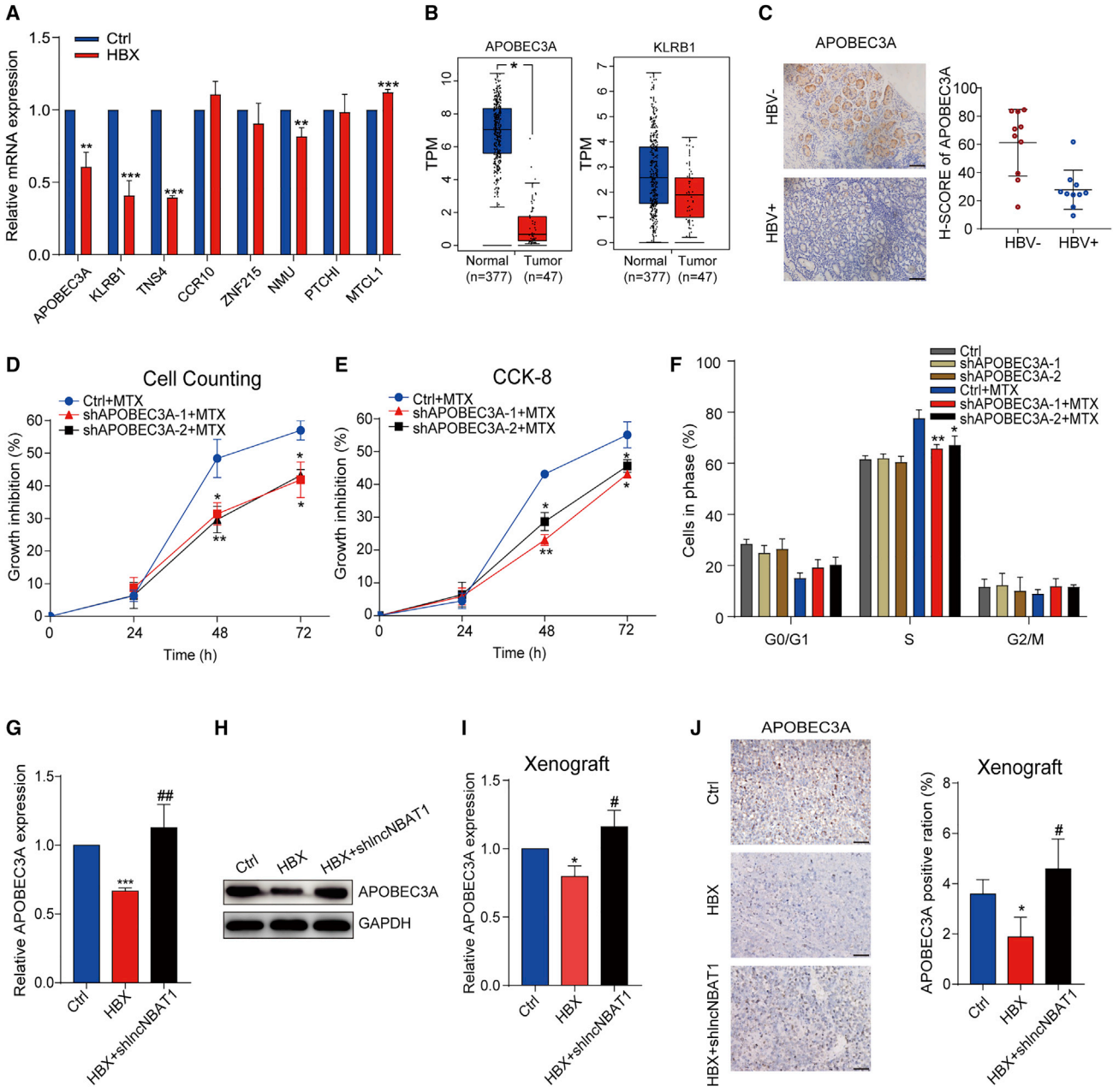

Figure 3. The HBX/lncNBAT1 axis suppresses expression of APOBEC3A *in vitro* and *in vivo*

(A) qRT-PCR analysis of the expression of chemoresistance-related genes in Ctrl and HBX-expressing cells. (B) Expression of APOBEC3A and KLRB1 in DLBCL tissue and normal tissue from the Gene Expression Profiling Interactive Analysis (GEPIA) database. (C) Immunohistochemical detection of APOBEC3A in DLBCL samples with or without HBV infection (left). The H score of APOBEC3A is shown (right). Scale bars, 100 μm. (D–F) Cell counting (D), CCK-8 (E), and flow cytometry (F) analyses revealed the effect of APBEC3A knockdown in HBX-expressing cells after MTX treatment (4.5 ng/mL). (G and H) qRT-PCR (G) and western blot (H) analyses of the expression of APOBEC3A in Ctrl cells, HBX-expressing cells, and HBX-expressing cells transfected with shlncNBAT1. * represents the significance of HBX versus Ctrl. # represents the significance of HBX + shlncNBAT1 versus HBX. (I) qRT-PCR analysis of the expression of APOBEC3A in xenograft tumors. * represents the significance of HBX versus Ctrl. # represents the significance of HBX + shlncNBAT1 versus HBX. (J) Immunohistochemical analysis of tumor sections from the indicated groups using anti-APOBEC3A (left). Histogram statistics for the positive cells of the indicated proteins are shown (right). * represents the significance of HBX versus Ctrl. # represents the significance of HBX + shlncNBAT1 versus HBX. Scale bars, 100 μm. The results were determined in triplicate, and the error bars represent the mean ± SD. */#$p < 0.05$, **/##$p < 0.01$, ***/###$p < 0.001$.

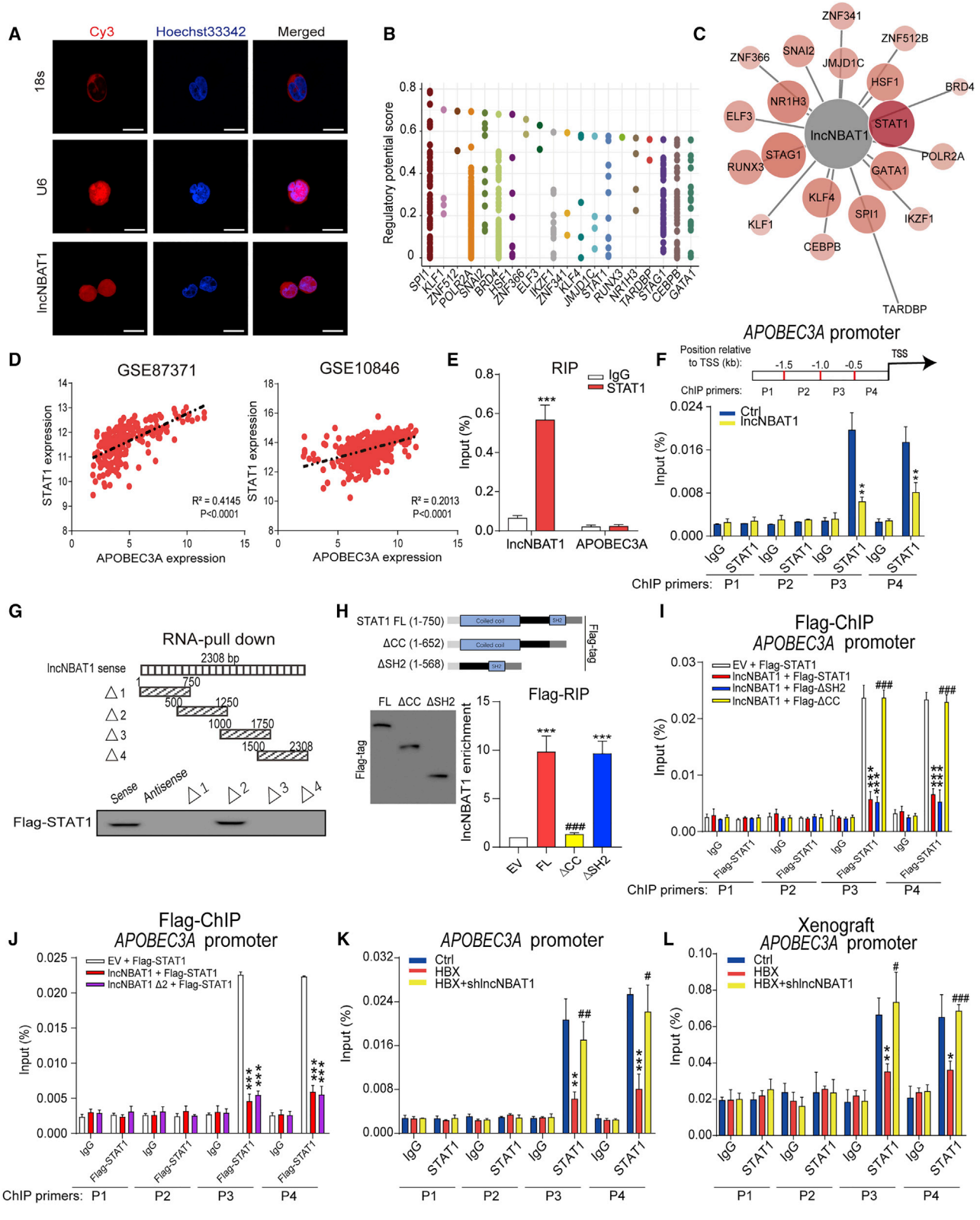

(legend on next page)

APOBEC3A, and this repression could be restored by lncNBAT1 inhibition in xenograft tumor tissue (Figures 3I and 3J). The results showing that the HBX/lncNBAT1 axis strictly regulated expression of APOBEC3A suggest that APOBEC3A might play important roles in HBX-induced chemoresistance in DLBCL.

lncNBAT1 binds STAT1 and impedes STAT1 enrichment at the *APOBEC3A* promoter

We next investigated how HBX/lncNBAT1 regulates APOBEC3A expression. Consistent with HBX overexpression, we found that overexpression of lncNBAT1 also significantly inhibited the mRNA and protein levels of APOBEC3A in SUDHL-4 cells (Figure S5A). lncNBAT1 was mainly distributed in the nucleus of SUDHL-4 cells and only existed in humans (Figures 4A, S6A, and S6B). Then we transfected HBX and lncNBAT1 into HEK293T cells to assess *APOBEC3A* gene promoter activity. Our results showed that introduction of lncNBAT1, but not HBX, significantly inhibited *APOBEC3A* gene promoter activity in a dose-dependent manner (Figure S5B). ChIP sequencing (ChIP-seq) data in the Cistrome DB database (http://dbtoolkit.cistrome.org/) were employed to predict the top 20 potential transcription factors (TFs) enriched at the *APOBEC3A* promoter region; the results are shown in Figure 4B. We further predicted the interaction of lncNBAT1 and potential TFs (http://bioinfo.bjmu.edu.cn/lncpro/), and the results showed that STAT1 might bind with lncNBAT1 (Figure 4C). According to the two independent DLBCL cohorts (GSE87371 and GSE10846), we found that expression of STAT1 was positively correlated with that of APOBEC3A (Figure 4D). The immunofluorescent staining showed that STAT1 was also colocalized in the nucleus with lncNBAT1, which confirmed the interaction of STAT1 and lncNBAT1 (Figure S7). Thus, we speculated that STAT1 might be involved in regulation of APOBEC3A expression by lncNBAT1. Using an RNA immunoprecipitation (RIP) assay, we confirmed that lncNBAT1 could bind to STAT1 and that overexpression of STAT1 could upregulate the mRNA and protein levels of APOBEC3A in SUDHL-4 cells (Figure S5C). An analysis using the Encyclopedia of DNA Elements (ENCODE) (https://www.encodeproject.org/) and ChIP assay indicated that STAT1 could bind to the promoter of the *APOBEC3A* gene and that its enrichment was remarkably decreased at the *APOBEC3A* promoter (−1.0 to −0.5 kb and −0.5 to 0 kb) following lncNBAT1 overexpression in SUDHL-4 cells (Figures 4F and S5D). To identify the STAT1-interacting region of lncNBAT1, we constructed vectors expressing full-length sense lncNBAT1 (sense), antisense lncNBAT1 (antisense), and four fragments of lncNBAT1 (Δ1, 1–750 nt; Δ2, 500–1,250 nt; Δ3, 1,000–1,750 nt; Δ4, 1,500–2,308 nt) combined with MS2bs elements, which were cotransfected with FLAG-STAT1 into HEK293T cells. Our results showed that the fragment of lncNBAT1 (500–1,250 nt) mainly mediated the interaction with STAT1 (Figure 4G). Next, we constructed truncated STAT1 and found that truncated STAT1 had the same overexpression efficiency as full-length STAT1 (Figure 4H). RIP assays with full-length or truncated STAT1 demonstrated that the coiled-coil domain of STAT1 was responsible for the interaction with lncNBAT1 (Figure 4H). Moreover, our findings indicated that the coiled-coil domain deletion mutant of STAT1, rather than the SH2 deletion mutant, failed to diminish binding of STAT1 at the promoter region of the *APOBEC3A* gene and that the fragment (500–1,250 nt) of lncNBAT1 was responsible for impeding STAT1 binding at the promoter of the *APOBEC3A* gene (Figures 4I and 4J). Additionally, we found that enrichment of STAT1 at −1.0 to −0.5 kb and −0.5 to 0 kb of the *APOBEC3A* promoter was also remarkably decreased upon HBX expression (Figure 4K). Furthermore, knockdown of lncNBAT1 restored the STAT1 enrichment at the *APOBEC3A* promoter region in HBX-overexpressing cells (Figure 4K). Consistently, ChIP-qPCR detection of tumor tissues removed after subcutaneous tumor formation found that HBX overexpression decreased enrichment of STAT1 at −1.0 to −0.5 kb and −0.5 to 0 kb of the *APOBEC3A* promoter and that this decrease was rescued by lncNBAT1 knockdown (Figure 4L). These results confirmed that HBX/lncNBAT1 negatively regulated APOBEC3A transcription by interfering with STAT1 binding at the promoter region of the *APOBEC3A* gene.

APOBEC3A serves as a downstream target of the HBX/lncNBAT1 axis

To study whether APOBEC3A was the downstream target of HBX/lncNBAT1 in DLBCL chemoresistance, we stably overexpressed APOBEC3A in HBX-expressing cells, and upregulation of APOBEC3A was

Figure 4. lncNBAT1 binds STAT1 and impedes STAT1 enrichment at the *APOBEC3A* promoter

(A) Representative image of FISH for lncNBAT1 (red) in SUDHL-4 cells. Nuclei were stained with Hoechst 33342 (blue). Scale bars, 50 μm. (B) ChIP-seq data from the Cistrome Data Browser database show the top 20 potential transcription factors (TFs) bound at the *APOBEC3A* promoter region. (C) The interaction of lncNBAT1 and potential TFs was predicted, and the results showed that lncNBAT1 and STAT1 had a strong potential interaction. (D) Pearson correlation analysis between STAT1 and APOBEC3A expression in the DLBCL cohorts (GSE87371 and GSE10846). (E) qRT-PCR analysis of the binding of lncNBAT1 and STAT1 with anti-STAT1 antibody in SUDHL-4 cells. APOBEC3A mRNA was not bound with lncNBAT1. (F) Enrichment of STAT1 at the promoter of the *APOBEC3A* gene in lncNBAT1-overexpressing cells compared with Ctrl cells. * represents the significance of lncNBAT1 versus Ctrl. (G) Western blot of FLAG-STAT1 in samples pulled down by full-length lncNBAT1 (sense), antisense lncNBAT1 (antisense), and four fragments of lncNBAT1 (Δ1, 1–750 nt; Δ2, 500–1,250 nt; Δ3, 1,000–1,750 nt; Δ4, 1,500–2,308 nt). (H) qRT-PCR analysis of the binding of lncNBAT1 and truncated STAT1 with anti-FLAG antibody in HEK293T cells. Western blot of the FLAG tag showed the expression of truncated STAT1. * represents the significance of Full length (FL) or ΔSH2 versus Empty Vector (EV). # represents the significance of ΔCC versus FL. (I) Enrichment of STAT1 at the promoter of the *APOBEC3A* gene in the groups of lncNBAT1-expressing cells with expression of wild-type or deletion mutant STAT1. * represents the significance of lncNBAT1 + FLAG-STAT1 or lncNBAT1 + FLAG-ΔSH2 versus EV + FLAG-STAT1. # represents the significance of lncNBAT1 + FLAG-ΔCC versus lncNBAT1 + FLAG-STAT1. (J) Enrichment of STAT1 at the promoter of the *APOBEC3A* gene in the groups of FLAG-STAT1-expressing cells with expression of lncNBAT1 or lncNBAT1 fragment Δ2. * represents the significance of lncNBAT1 + FLAG-STAT1 or lncNBAT1 Δ2 + FLAG-STAT1 versus EV + FLAG-STAT1. (K and L) Enrichment of STAT1 at the promoter of the *APOBEC3A* gene in the Ctrl cells, HBX-expressing cells, and HBX-expressing cells transfected with shlncNBAT1 (K) or in xenograft tumors (L). * represents the significance of HBX versus Ctrl. # represents the significance of HBX + shlncNBAT1 versus HBX. The results were determined in triplicate, and the error bars represent the mean ± SD. */#$p < 0.05$, **/##$p < 0.01$, ***/###$p < 0.001$.

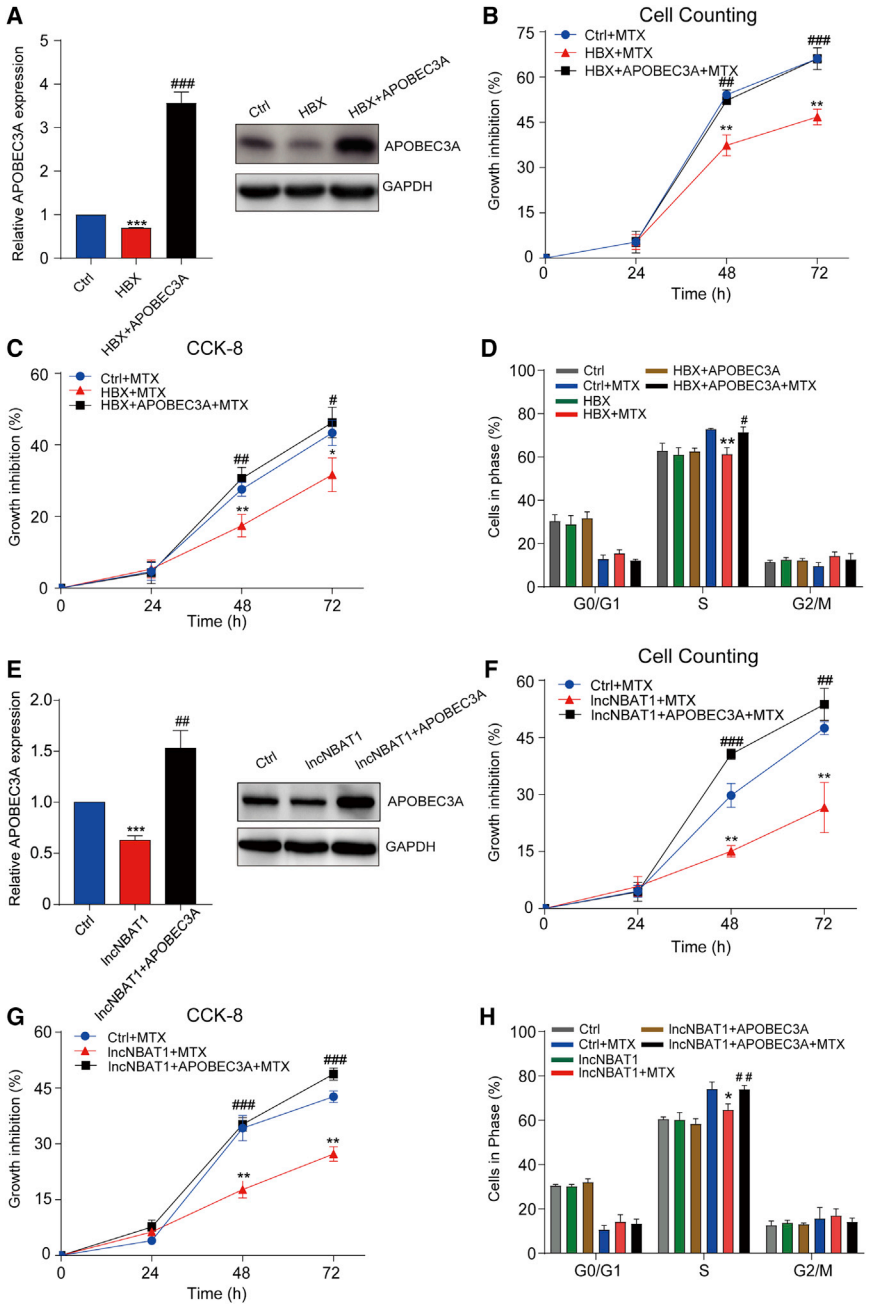

Figure 5. APOBEC3A serves as a downstream target of the HBX/lncNBAT1 axis

(A) The APOBEC3A expression level was detected in Ctrl cells, HBX cells, and HBX + APOBEC3A cells via qRT-PCR (left) and western blot (right). (B–D) Cell counting (B), CCK-8 (C), and flow cytometry (D) analyses revealed the effect of APOBEC3A overexpression in HBX-expressing cells after MTX treatment (4.5 ng/mL). * represents the significance of HBX + MTX versus Ctrl + MTX. # represents the significance of HBX + APOBEC3A + MTX versus HBX + MTX. (E) The APOBEC3A expression level was analyzed in control, lncNBAT1, and lncNBAT1+ APOBEC3A cells via qRT-PCR (left) and western blotting (right). (F–H) Cell counting (F), CCK-8 (G), and flow cytometry (H) analyses revealed the effect of APOBEC3A overexpression in lncNBAT1-overexpressing cells after MTX treatment (4.5 ng/mL). * represents the significance of lncNBAT1 + MTX versus Ctrl + MTX. # represents the significance of lncNBAT1+ APOBEC3A + MTX versus lncNBAT1 + MTX. The results were determined in triplicate, and the error bars represent the mean ± SD. */#p < 0.05, **/##p < 0.01, ***/###p < 0.001.

confirmed (Figure 5A). We found that overexpression of APOBEC3A reversed attenuation of HBX on cell proliferation inhibition and S phase arrest induced by MTX treatment (Figures 5B–5D). Similarly, we overexpressed APOBEC3A in lncNBAT1-expressing cells, and overexpression of APOBEC3A was confirmed by RT-PCR and western blotting (Figure 5E). As expected, overexpression of APOBEC3A significantly restored growth inhibition and S phase arrest of MTX weakened by lncNBAT1 overexpression in SUDHL-4 cells (Figures 5F–5H). Our data indicated that APOBEC3A serves as a functional target of HBX/lncNBAT1-induced chemoresistance to S phase arrest chemotherapy.

lncNBAT1/APOBEC3A is associated with DLBCL clinical characteristics and poor prognosis

When we analyzed the correlation between lncNBAT1/APOBEC3A and clinical outcomes in individuals with DLBCL, using DLBCL datasets from the Gene Expression Omnibus (GEO) database, we found that expression of lncNBAT1 was significantly higher in tumor tissue than in normal tissue (Figure 6A) and that lncNBAT1 expression was significantly higher in tumor samples from individuals with DLBCL at advanced stages (stages II/IV) than in those from an early stage (stage I) (Figure 6B). Additionally, we found that expression of lncNBAT1 was negatively correlated with that of APOBEC3A (Figure 6C). Kaplan-Meier survival analysis of the DLBCL cohort (The National Cancer Institute`s Center for Cancer Research [NCICCR]) showed that individuals with DLBCL with high lncNBAT1 expression had a significantly shorter overall survival (OS) (Figure 6D). The finding that higher lncNBAT1 expression was associated with shorter OS of individuals with DLBCL was also confirmed by analyzing the survival of the DLBCL cohort (GSE10846) (Figure S8A). Consistent with inhibition of APOBEC3A expression by lncNBAT1, we found that low expression of APOBEC3A was associated with reduced OS, according to two independent DLBCL cohorts (NCICCR and GSE4475) (Figures 6E and S8B). To investigate the clinical

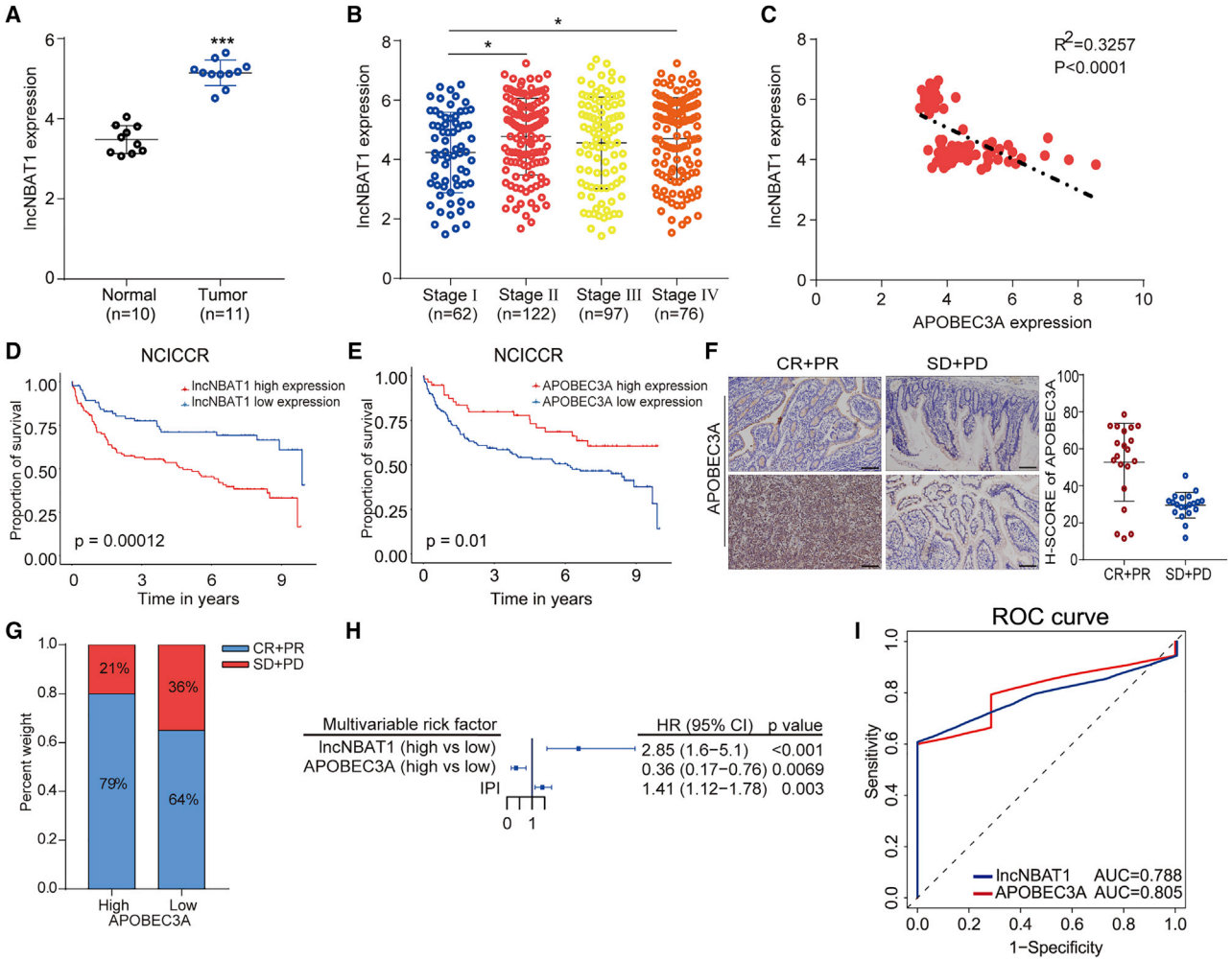

Figure 6. LncNBAT1/APOBEC3A is associated with DLBCL clinical characteristics and poor prognosis

(A) Expression of lncNBAT1 in DLBCL tissue and normal tissue (GSE12453 and GSE65135). (B) The lncNBAT1 expression level in stage I, II, III, and IV DLBCL cohorts (GSE10846). (C) Pearson correlation analysis between lncNBAT1 and APOBEC3A expression using the DLBCL cohorts (GSE87371). (D) Kaplan-Meier analysis of OS of individuals with DLBCL in the NCICCR database. A log rank test was used to determine the statistical significance between the low lncNBAT1 expression group and the high lncNBAT1 expression group. (E) Survival was analyzed and compared between individuals with high and low APOBEC3A expression in the NCICCR using the Kaplan-Meier method. (F) Immunohistochemical detection of APOBEC3A in individuals with DLBCL with disease control (complete response [CR], partial response [PR], stable disease [SD], and progressive disease [PD]; left). The H score of APOBEC3A is shown (right). Scale bars, 100 μm. (G) Percentage of individuals with DLBCL who responded to chemotherapy in the high and low APOBEC3A expression groups. (H) Multivariate Cox regression of clinicopathological variables and lncNBAT1/APOBEC3A expression levels in individuals with DLBCL. (I) ROC analysis of the OS of lncNBAT1 (area under the ROC curve [AUC] = 0.788) and APOBEC3A (AUC = 0.805) as individual biomarkers. The results were determined in triplicate, and the error bars represent the mean ± SD. *$p < 0.05$, **$p < 0.01$, ***$p < 0.001$.

implications of APOBEC3A in DLBCL, we performed immunohistochemistry (IHC) staining for APOBEC3A in DLBCL tissue and found that APOBEC3A expression was decreased in individuals with DLBCL with poorer chemotherapy outcomes (stable disease and progressive disease [PD]) than in those with better chemotherapy outcomes (complete response [CR] and partial response [PR]) (Figure 6F). Furthermore, we explored the correlation between APOBEC3A expression and the disease control rate in individuals with DLBCL and found that those with low expression of APOBEC3A had fewer benefits from standard chemotherapy (Figure 6G). To evaluate the pathological and clinical value of lncNBAT1 and APOBEC3A, we performed univariate and multivariate regression analyses of the DLBCL cohort (NCICCR) and found that expression of lncNBAT1/APOBEC3A served as an independent prognostic factor for individuals with DLBCL (Figures 6H and S8C). Moreover, receiver operating characteristic (ROC) curve analysis also showed the potential of lncNBAT1/APOBEC3A as a marker of poor prognosis in DLBCL (Figure 6I). These results demonstrated that lncNBAT1/APOBEC3A was clearly associated with the outcomes of individuals with DLBCL.

DISCUSSION

Chemoresistance, a multifactorial phenomenon, has been the major obstacle for effective treatment of DLBCL,[3–5] where multiple factors, such as methylase KDM6B,[29] exosomal CA1,[30] and phosphatidylinositol 3-kinase (PI3K)/AKT signaling,[31] have been proven to be closely related to the sensitivity of chemotherapeutic drugs in DLBCL treatment. HBV infection has been considered an independent factor for chemotherapy resistance and poor prognosis in individuals with DLBCL,[7,10,19] but the underlying mechanisms have not been clarified. Our previous study indicated that the core component of HBV (HBX) inhibited the DNA damage response pathway, leading to chemoresistance in DLBCL.[22] A recent study identified that lncNBAT1 plays important regulatory roles in tumorigenesis,[32,33] but the distinct roles and mechanisms of lncNBAT1 in DLBCL chemoresistance remain unknown. Our results found that lncNBAT1 could be directly upregulated by HBX and was closely related to DLBCL progression and poor survival. Overexpression of lncNBAT1 mimicked HBX-induced resistance to S phase arrest drugs, and knockdown of lncNBAT1 significantly relieved the resistance caused by HBX overexpression in DLBCL. Our findings identified, for the first time, that lncNBAT1 potentially mediates the chemoresistance induced by HBV infection in DLBCL, which could serve as a new molecular target for restoration of sensitivity to chemotherapy drugs in HBV-infected individuals with DLBCL.

APOBEC3A can hinder infection with retroviruses in humans and plays an important role in the immune response.[34] Previous studies have shown that APOBEC3A can inhibit HBV infection by deaminating covalently closed circular DNA (cccDNA) and causing formation of apurinic/apyrimidinic (AP) sites that are recognized by cellular AP endonucleases, leading to cccDNA digestion.[35,36] On the other hand, HBV can inhibit APOPEC3A expression by promoting UBE2L3-mediated APOPEC3A protein degradation, which maintains the stability of HBV cccDNA and continuously infects host cells.[37] A recent study found that the activity of cytidine deaminase induced by APOBEC3A might be the main reason for the increasing rate of genome mutagenesis and unique mutations by analyzing the genetic profiles of HBV-infected individuals with DLBCL,[21] suggesting that APOBEC3A may be a pivotal regulator of the progression of HBV-infected individuals with DLBCL. APOBEC3A can activate the DNA damage signal γH2AX through its deaminase activity, inducing cell cycle arrest and DNA damage repair.[38] Several studies have shown that expression of APOBEC3A is correlated with the sensitivity of pancreatic cancer to bromodomain and extraterminal family of proteins (BET) inhibitors and CDK4/6 inhibitors.[39] Additionally, APOBEC3A can activate replication checkpoints, improving the therapeutic effect of ATR and Chk1 inhibitors in human acute myeloid leukemia.[40] Our study found that APOBEC3A was transcriptionally downregulated by the HBX/lncNBAT1 axis in DLBCL. The decreased expression of APOBEC3A induced resistance to chemotherapeutic drugs, whereas its overexpression relieved the chemoresistance caused by HBX and lncNBAT1, indicating that APOBEC3A served as an uncovered downstream functional target of HBX/lncNBAT1-induced chemotherapy resistance. We thus discovered a new mechanism of lncRNA-mediated downregulation of APOBEC3A after HBV infection and a novel function of APOBEC3A in HBV infection-induced chemotherapy resistance and poor prognosis of individuals with DLBCL.

Emerging evidence shows that lncRNAs execute their important regulatory roles in chemotherapy resistance via transcriptional or post-transcriptional regulation of target genes.[24] The lncRNA TUG1 could lead to resistance to chemotherapeutic agents in esophageal cancer by promoting EZH2 enrichment at the *PDCD4* promoter region and inhibiting expression of the tumor suppressor PDCD4.[41] The lncRNA UCA1 causes chemotherapy resistance in breast cancer through binding with miR-18a and alleviating its inhibition of HIF1α.[42] Recent studies also found that the lncRNA MALAT-1, highly expressed in DLBCL cells, can reduce sensitivity to the chemotherapy drug Adriamycin by inhibiting autophagy-related proteins.[43] The expression levels of the lncRNA HULC and PEG10 were positively correlated with the chemotherapy effect of R-CHOP treatment in individuals with DLBCL,[44,45] but the link between lncRNA and HBV-induced DLBCL chemoresistance is poorly understood. lncNBAT1 has been proven to interact with EZH2 and suppress expression of RE1 silencing transcription factor (REST) and SOX9 to inhibit cell proliferation and invasion of neuroblastoma.[46] lncNBAT1 interacts with miR-21 and upregulates the downstream genes of miR-21, including PTEN, PDCD4, TPM1, and RECK, to inhibit osteosarcoma growth and metastasis.[47] Additionally, lncNBAT1 can act as a decoy of IGF2BP1 and inhibit the interaction between IGF2BP1 and c-Myc mRNA, suppressing the stability of c-Myc mRNA.[48] A recent study revealed that lncNBAT1 can suppress ATG7 expression and autophagy, which results in resistance to cisplatin in non-small cell lung cancer.[32] Our results revealed a new function of lncNBAT1 in regulating resistance to MTX and Ara-C therapy in HBX-expressing DLBCL cells. Nuclearly distributed lncNBAT1 mechanically bound to STAT1 and significantly reduced enrichment of STAT1 at the *APOBEC3A* gene promoter region. This research revealed a mechanism by which the lncNBAT1/STAT1 interaction regulates APOBEC3A expression and chemotherapy resistance in HBV-infected DLBCLs.

MATERIALS AND METHODS

Cell culture

The DLBCL cell lines SUDHL-4, DB, and 293FT were purchased from the American Type Culture Collection (ATCC; Manassas, VA, USA). All cell culture media were supplemented with 10% fetal bovine serum (FBS) (Gibco Life Technologies, Carlsbad, CA, USA), and the cells were maintained at 37°C with 5% CO_2 in a humidified incubator.

In vitro cell growth assay and chemotherapeutic agents

In vitro cell growth assays were performed using a cell counting assay or CCK-8 assay. For the cell counting assay, cells (8×10^4) were seeded in a 12-well plate, and the indicated amounts of chemotherapeutic agents were added. Cell numbers were measured by cell

counter after 24, 48, and 72 h. For the CCK-8 assay, cells (3×10^3) were seeded in 96-well plates with the indicated amounts of chemotherapeutic agents added. Then, 20 μL of CCK-8 solution was added to each well at 37°C for 2 h, and the absorbance (450 nm) was measured with a SpectraMax iD3 after treatment with chemotherapeutic agents for 24, 48, and 72 h. The following chemotherapeutic agents were used: MTX (Pfizer, Shanghai, China) and Ara-C (Pharmacia, Shanghai, China).

RNA sequencing and microarray data analysis

DLBCL gene expression data were obtained from the NCICCR and GEO databases. Independent datasets from GSE10846, GSE56315, GSE4475, GSE87371, GSE12453, GSE23501 and GSE65135 were analyzed in this study. The RNA-sequencing files and microarray files were downloaded from the NCICCR and GEO databases, respectively.

Flow cytometry analysis

The cells were harvested after adding chemotherapeutic agents for 48 h and fixed in 1 mL of precooled 70% ethanol for at least 8 h. The cells were stained with propidium iodide/RNase (Beyotime, Shanghai, China) at 37°C for 30 min in the dark. Cell cycle distribution was evaluated by flow cytometry using a FACSCalibur (BD Biosciences, Franklin Lakes, NJ, USA) and analyzed by FlowJo software (version 7.6).

Tumor xenografts

Five-week-old NOD-SCID mice were purchased from the National Resource Center for Rodent Laboratory Animals of China. Control cells, HBX-expressing SUDHL-4 cells, and HBX-expressing SUDHL-4 cells with shlncNBAT1 (1×10^7 cells each) suspended in 100 μL of one part Matrigel (BD, 356234) and two parts DMEM were subcutaneously injected into the left and right thighs of the mice, respectively. On day 14 after tumor cell injection, the mice were monitored to assess the tumor volume using the formula 1/2 (length × width^2) and injected intraperitoneally with MTX (10 mg/kg) every 3 days until day 26. The xenograft tumors were harvested on day 26 after injection. All experiments were carried out as approved by the Institutional Animal Care and Use Committee of Tongji University.

ChIP

The ChIP assay was performed as described previously.[49] The cells were crosslinked with 1% formaldehyde for 10 min and quenched with 0.25 M glycine for 5 min at room temperature to further lyse them. The cell pellet was lysed in cell lysis buffer (5 mM PIPES [pH 8.0], 85 mM KCl, and 0.5% NP40) and nucleus lysis buffer (50 mM Tris [pH 8.1], 10 mM EDTA, 0.75% SDS, and 50 mM PMSF), and then these samples were sonicated using an M220 focused ultrasonicator (Covaris) to generate 500- to 750-bp fragments. Fragmented chromatin was centrifuged at 12,000 rpm for 10 min, and the supernatants were diluted in dilution buffer (16.7 mM Tris-HCl [pH 8.1], 167 mM NaCl, 0.01% SDS, 1.2 mM EDTA, and 1.1% Triton X-100). Immunoprecipitation was performed overnight by rotating samples at 4°C with magnetic beads (ChIP-grade protein G beads, catalog number 9006s, Cell Signaling Technology) prebound with 3 μg of antibody. The beads were washed once each with TSE buffer I (20 mM Tris [pH 8.1], 150 mM NaCl, 0.1% SDS, 1% Triton X-100, and 2 mM EDTA), TSE buffer II (20 mM Tris [pH 8.1], 500 mM NaCl, 0.1% SDS, 1% Triton X-100, and 2 mM EDTA), wash buffer III (10 mM Tris [pH 8.1], 250 mM LiCl, 1% deoxycholate, 1% NP40, and 1 mM EDTA), and TE buffer (10 mM Tris [pH 8.1] and 1 mM EDTA). All washes took place on a rotator for 5 min at 4°C. Beads were treated with 300 mL of elution buffer (100 mM $NaHCO_3$ and 1% SDS). Then 30 mL of 5 M NaCl was added to the elution, and the sample was reverse crosslinked overnight at 65°C. Samples were treated with 1.5 mL of RNase A at 37°C for 1 h, and then 3 mL of Proteinase K (20 μg/mL) was added at 55°C for 1 h. DNA was then purified with phenol-chloroform (Sangon Biotech). The following antibodies were used in ChIP experiments: anti-HBX (MA1081, Thermo Fisher Scientific), anti-STAT1 (9172, Cell Signaling Technology), anti-FLAG (GNI4110, GNI), and anti-immunoglobulin G (IgG)-Rb (2729, Cell Signaling Technology). The immunoprecipitated DNA and input DNA were used as templates for qRT-PCR.

GSEA

GSEA was employed to identify gene sets correlated with lncNBAT1 in DLBCL. Gene expression profiles of DLBCL were obtained from the GSE56315 dataset. DLBCL samples were divided into two groups according to expression of lncNBAT1 (high expression, the top 10% samples; low expression, the bottom 10% samples). The GSEA v.3.0 tool was used to explore the distribution of members of the gene sets from the Molecular Signatures Database (MSigDB).[50]

Luciferase reporter assay

Luciferase reporters were generated by cloning the *lncNBAT1* promoter (−3,000 to 0 bp) or *APOBEC3A* promoter (−2,000 to 0 bp) into the pGL3-basic vector (Promega). Then HEK293T cells (3×10^4 in each well of a 24-well plate) were cotransfected with 200 ng of luciferase reporters, 1 ng of the internal control vector (*Renilla*), and 200 ng of the indicated plasmids, with 1 μL of FuGENE HD reagent. Cell lysates were harvested 48 h after transfection. Luciferase activities were examined using the Dual-Luciferase Reporter Assay System (Promega). Briefly, cultured cells were rinsed in 1× PBS. 100 mL of 1× passive lysis buffer (Promega) was added, and the culture vessel was gently shaken for 15 min at room temperature. Then 10–20 μL of lysis buffer was used to measure the firefly luciferase activity after adding 100 μL of luciferase assay reagent II (Promega), and the *Renilla* luciferase activity was measured after dispensing 100 μL of Stop & Glo reagent (Promega) with a Tecan Infinite 200 Pro instrument.

RIP

RIP was performed as described previously.[44] A total of 5×10^6 cells were lysed with lysate buffer. Protein A magnetic beads (161-4013, Bio-Rad) and protein G magnetic beads (161-4023, Bio-Rad) were incubated with 3 μg of antibodies and rotated for at least 6 h. Lysates

were added to the prepared beads in RIP buffer and rotated overnight for immunoprecipitation. Finally, RNA was extracted with RNAiso Plus reagent. The antibodies in the RIP assay were as follows: anti-STAT1, anti-FLAG, and anti-IgG-Rabbit (Rb).

Fluorescence *in situ* hybridization

SUDHL-4 cells were rinsed briefly in 1× PBS and then fixed in 4% paraformaldehyde for 10 min at room temperature. Cells were permeabilized in 1× PBS containing 0.5% Triton X-100 for 5 min at 4°C, then washed in 1× PBS for 5 min. Two hundred microliters of prehybridization buffer was added at 37°C for 30 min. Hybridization was carried out with a fluorescence *in situ* hybridization (FISH) probe in a moist chamber at 37°C in the dark overnight using the Ribo Fluorescent *In Situ* Hybridization Kit (C10910, RiboBio). The slides were washed three times with wash buffer I (4× saline sodium citrate [SSC] with 0.1% Tween 20), once each with wash buffer II (2× SSC) and wash buffer III (1× SSC) at 42°C in the dark for 5 min, and once with 1× PBS at room temperature. Then the SUDHL-4 cells were stained with Hoechst 33342 in the dark for 10 min. The lncNBAT1-cy3 FISH probes (LNC1CM001) were designed and synthesized by RiboBio. U6 FISH probes (LNC 110101, RiboBio) and 18S FISH probes (LNC110102, RiboBio) were used as the nuclear and cytoplasmic controls, respectively. All images were obtained with a fluorescence or confocal microscope (Nikon).

MS2bp-Yellow Fluorescent Protein (YFP) RNA pull-down

The MS2bp-MS2bs-based RIP assay was performed as described previously.[49] Briefly, 5 × 10^6 HEK293T cells were seeded into 100-mm plates and cotransfected with 4 μg of MS2bs overexpression vectors (pcDNA3-MS2bs) or blank control vectors with *Renilla* luciferase inserts (pcDNA3-MS2bs-RL), 5 μg of the MS2bp-YFP overexpression plasmid, and 4 μg of pcDNA overexpression vectors with 40 μL of FuGENE HD (Roche). After 48 h, the cells were lysed with RIP buffer (100 mM KCl, 5 mM $MgCl_2$, 10 mM HEPES [pH 7.0], 0.5% NP-40, and 1 mM dithiothreitol) for 30 min on ice to facilitate lysis. The proteins were immunoprecipitated using control IgG (2729, Cell Signaling Technology) or anti-GFP antibody (ab290, Abcam), which was able to recognize YFP. The complexes of RNA and RNA-binding proteins were treated with RNAiso (Takara) to purify the RNA or SDS lysis buffer for western blot analysis.

Western blotting and immunohistochemistry

Western blotting and immunohistochemistry were performed according to standard procedures.[51] The following antibodies were used: anti-HBX (ab39716, Abcam), anti-STAT1 (9172, Cell Signaling Technology), anti-glyceraldehyde-3-phosphate dehydrogenase (GAPDH) (sc-47724, Santa Cruz Biotechnology), anti-APOBEC3A (AP1354a, Abgent), anti-FLAG (GNI4110, GNI), horseradish peroxidase (HRP)-Mouse (Ms) (7074, Cell Signaling Technology), and HRP-Rb (7076, Cell Signaling Technology).

Statistical analysis

Statistical analyses were performed using GraphPad Prism 7 software and R (version 3.6). The results were from triplicate experiments, and the data are presented as the mean or mean ± SD. The significance of mean values was determined by unpaired two-tailed Student's t test. The survival times of different groups of individuals were analyzed using the R package "survival." Univariate and multivariate Cox analyses on the individual clinical variables were done using the R package "survival." Time-dependent ROC curves were generated, and the area under the ROC curve (AUC) was used to assess the prognostic performance via the R package "survivalROC."

SUPPLEMENTAL INFORMATION

Supplemental information can be found online at https://doi.org/10.1016/j.omtn.2022.01.015.

ACKNOWLEDGMENTS

This study was supported by grants from the Ministry of Science and Technology (2018YFA0800100), the National Natural Science Foundation of China (grants 81970178, 31830059, 31970599, 32170575, and 31721003), the Shanghai Rising-Star Program (20QA1409600), and Fundamental Research Funds for the Central Universities (22120210060 and 22120210438). We thank Prof. Jinyu Wu (Wenzhou Medical University) for technical support with data analysis.

AUTHOR CONTRIBUTIONS

J.L. and Y.C. performed the experiments. X.G., J.C., and J.K. conceived the study. J.L., X.G., and J.K. wrote and revised the manuscript. X.G., X.B., X.X., T.H., A.T., N.L., Y.X., and Q.S. provided experimental support. All authors read and approved the final manuscript.

DECLARATION OF INTERESTS

The authors declare no competing interests.

REFERENCES

1. Teras, L.R., DeSantis, C.E., Cerhan, J.R., Morton, L.M., Jemal, A., and Flowers, C.R. (2016). 2016 US lymphoid malignancy statistics by World Health Organization subtypes. CA Cancer J. Clin. *66*, 443–459.

2. Liu, Y., and Barta, S.K. (2019). Diffuse large B-cell lymphoma: 2019 update on diagnosis, risk stratification, and treatment. Am. J. Hematol. *94*, 604–616.

3. Camicia, R., Winkler, H.C., and Hassa, P.O. (2015). Novel drug targets for personalized precision medicine in relapsed/refractory diffuse large B-cell lymphoma: a comprehensive review. Mol. Cancer *14*, 207.

4. Roschewski, M., Dunleavy, K., and Wilson, W.H. (2012). Diffuse large B cell lymphoma: molecular targeted therapy. Int. J. Hematol. *96*, 552–561.

5. de Jong, M.R.W., Langendonk, M., Reitsma, B., Herbers, P., Lodewijk, M., Nijland, M., van den Berg, A., Ammatuna, E., Visser, L., and van Meerten, T. (2020). WEE1 inhibition synergizes with CHOP chemotherapy and radiation therapy through induction of premature mitotic entry and DNA damage in diffuse large B-cell lymphoma. Ther. Adv. Hematol. *11*. https://doi.org/10.1177/2040620719898373.

6. Cheng, C.L., Huang, S.C., Chen, J.H., Wei, C.H., Fang, W.Q., Su, T.H., Yuan, C.T., Liu, J.H., Chuang, M.K., and Tien, H.F.. Hepatitis B surface antigen positivity is an independent unfavorable prognostic factor in diffuse large B-cell lymphoma in the rituximab era. Oncologist: 10 793

7. Deng, L., Song, Y., Young, K.H., Hu, S., Ding, N., Song, W., Li, X., Shi, Y., Huang, H., Liu, W., et al. (2015). Hepatitis B virus-associated diffuse large B-cell lymphoma: unique clinical features, poor outcome, and hepatitis B surface antigen-driven origin. Oncotarget *6*, 25061–25073.

8. Marcucci, F., and Mele, A. (2011). Hepatitis viruses and non-Hodgkin lymphoma: epidemiology, mechanisms of tumorigenesis, and therapeutic opportunities. Blood *117*, 1792–1798.

9. Chen, J., Wang, J., Yang, J., Zhang, W., Song, X., and Chen, L. (2013). Concurrent infection of hepatitis B virus negatively affects the clinical outcome and prognosis of patients with non-Hodgkin's lymphoma after chemotherapy. PLoS ONE *8*, e69400.

10. Kim, J.H., Bang, Y.J., Park, B.J., Yoo, T., Kim, C.W., Kim, T.Y., Heo, D.S., Lee, H.S., and Kim, N.K. (2002). Hepatitis B virus infection and B-cell non-Hodgkin's lymphoma in a hepatitis B endemic area: a case-control study. Jpn. J. Cancer Res. *93*, 471–477.

11. Takai, S., Tsurumi, H., Ando, K., Kasahara, S., Sawada, M., Yamada, T., Hara, T., Fukuno, K., Takahashi, T., Oyama, M., et al. (2005). Prevalence of hepatitis B and C virus infection in haematological malignancies and liver injury following chemotherapy. Eur. J. Haematol. *74*, 158–165.

12. Chen, M.H., Hsiao, L.T., Chiou, T.J., Liu, J.H., Gau, J.P., Teng, H.W., Wang, W.S., Chao, T.C., Yen, C.C., and Chen, P.M. (2008). High prevalence of occult hepatitis B virus infection in patients with B cell non-Hodgkin's lymphoma. Ann. Hematol. *87*, 475–480.

13. Stanaway, J.D., Flaxman, A.D., Naghavi, M., Fitzmaurice, C., Vos, T., Abubakar, I., Abu-Raddad, L.J., Assadi, R., Bhala, N., Cowie, B., et al. (2016). The global burden of viral hepatitis from 1990 to 2013: findings from the Global Burden of Disease Study 2013. Lancet *388*, 1081–1088.

14. El-Serag, H.B. (2012). Epidemiology of viral hepatitis and hepatocellular carcinoma. Gastroenterology *142*, 1264.

15. Schweitzer, A., Horn, J., Mikolajczyk, R.T., Krause, G., and Ott, J.J. (2015). Estimations of worldwide prevalence of chronic hepatitis B virus infection: a systematic review of data published between 1965 and 2013. Lancet *386*, 1546–1555.

16. Tarocchi, M., Polvani, S., Marroncini, G., and Galli, A. (2014). Molecular mechanism of hepatitis B virus-induced hepatocarcinogenesis. World J. Gastroenterol. *20*, 11630–11640.

17. Ching, R.H.H., Sze, K.M.F., Lau, E.Y.T., Chiu, Y.T., Lee, J.M.F., Ng, I.O.L., and Lee, T.K.W. (2017). C-terminal truncated hepatitis B virus X protein regulates tumorigenicity, self-renewal and drug resistance via STAT3/Nanog signaling pathway. Oncotarget *8*, 23507–23516.

18. Pontisso, P., Vidalino, L., Quarta, S., and Gatta, A. (2008). Biological and clinical implications of HBV infection in peripheral blood mononuclear cells. Autoimmun. Rev. *8*, 13–17.

19. Wang, F., Yuan, S., Teng, K.Y., Garcia-Prieto, C., Luo, H.Y., Zeng, M.S., Rao, H.L., Xia, Y., Jiang, W.Q., Huang, H.Q., et al. (2012). High hepatitis B virus infection in B-cell lymphoma tissue and its potential clinical relevance. Eur. J. Cancer Prev. *21*, 261–267.

20. El-Sayed, G.M., Mohamed, W.S., Nouh, M.A., Moneer, M.M., and El-Mahallawy, H.A. (2006). Viral genomes and antigen detection of hepatitis B and C viruses in involved lymph nodes of Egyptian non-Hodgkin's lymphoma patients. Egypt. J. Immunol. *13*, 105–114.

21. Ren, W., Ye, X., Su, H., Li, W., Liu, D., Pirmoradian, M., Wang, X., Zhang, B., Zhang, Q., Chen, L., et al. (2018). Genetic landscape of hepatitis B virus-associated diffuse large B-cell lymphoma. Blood *131*, 2670–2681.

22. Zhao, X., Guo, X., Xing, L., Yue, W., Yin, H., He, M., Wang, J., Yang, J., and Chen, J. (2018). HBV infection potentiates resistance to S-phase arrest-inducing chemotherapeutics by inhibiting CHK2 pathway in diffuse large B-cell lymphoma. Cell Death Dis. *9*, 61.

23. Iyer, M.K., Niknafs, Y.S., Malik, R., Singhal, U., Sahu, A., Hosono, Y., Barrette, T.R., Prensner, J.R., Evans, J.R., Zhao, S., et al. (2015). The landscape of long noncoding RNAs in the human transcriptome. Nat. Genet. *47*, 199–208.

24. Schmitt, A.M., and Chang, H.Y. (2016). Long noncoding RNAs in cancer pathways. Cancer Cell *29*, 452–463.

25. Xie, C., Zhang, L.Z., Chen, Z.L., Zhong, W.J., Fang, J.H., Zhu, Y., Xiao, M.H., Guo, Z.W., Zhao, N., He, X., et al. (2020). A hMTR4-PDIA3P1-miR-125/124-TRAF6 regulatory Axis and its function in NF kappa B signaling and chemoresistance. Hepatology *71*, 1660–1677.

26. Niu, Y., Ma, F., Huang, W., Fang, S., Li, M., Wei, T., and Guo, L. (2017). Long non-coding RNA TUG1 is involved in cell growth and chemoresistance of small cell lung cancer by regulating LIMK2b via EZH2. Mol. Cancer *16*, 5.

27. Verma, A., Jiang, Y., Du, W., Fairchild, L., Melnick, A., and Elemento, O. (2015). Transcriptome sequencing reveals thousands of novel long non-coding RNAs in B cell lymphoma. Genome Med. *7*, 110.

28. Song, Y., Gao, F., Peng, Y., and Yang, X. (2020). Long non-coding RNA DBH-AS1 promotes cancer progression in diffuse large B-cell lymphoma by targeting FN1 via RNA-binding protein BUD13. Cell Biol. Int. *44*, 1331–1340.

29. Mathur, R., Sehgal, L., Havranek, O., Köhrer, S., Khashab, T., Jain, N., Burger, J.A., Neelapu, S.S., Davis, R.E., and Samaniego, F. (2017). Inhibition of demethylase KDM6B sensitizes diffuse large B-cell lymphoma to chemotherapeutic drugs. Haematologica *102*, 373–380.

30. Feng, Y., Zhong, M., Tang, Y., Liu, X., Liu, Y., Wang, L., and Zhou, H. (2020). The role and underlying mechanism of exosomal CA1 in chemotherapy resistance in diffuse large B cell lymphoma. Mol. Ther. Nucleic Acids *21*, 452–463.

31. Chen, J.F., Ge, X.W., Zhang, W., Ding, P.P., Du, Y.Q., Wang, Q., Li, L., Fang, L., Sun, Y.J., Zhang, P.Z., et al. (2020). PI3K/AKT inhibition reverses R-CHOP resistance by destabilizing SOX2 in diffuse large B cell lymphoma. Theranostics *10*, 3151–3163.

32. Zheng, T., Li, D., He, Z., Feng, S., and Zhao, S. (2018). Long noncoding RNA NBAT1 inhibits autophagy via suppression of ATG7 in non-small cell lung cancer. Am. J. Cancer Res. *8*, 1801–1811.

33. Xue, S., Li, Q.W., Che, J.P., Guo, Y., Yang, F.Q., and Zheng, J.H. (2015). Decreased expression of long non-coding RNA NBAT-1 is associated with poor prognosis in patients with clear cell renal cell carcinoma. Int. J. Clin. Exp. Pathol. *8*, 3765–3774.

34. Henry, M., Terzian, C., Peeters, M., Wain-Hobson, S., and Vartanian, J.P. (2012). Evolution of the primate APOBEC3A cytidine deaminase gene and identification of related coding regions. PLoS ONE *7*, e30036.

35. Stenglein, M.D., Burns, M.B., Li, M., Lengyel, J., and Harris, R.S. (2010). APOBEC3 proteins mediate the clearance of foreign DNA from human cells. Nat. Struct. Mol. Biol. *17*, 222–229.

36. Lucifora, J., Xia, Y., Reisinger, F., Zhang, K., Stadler, D., Cheng, X., Sprinzl, M.F., Koppensteiner, H., Makowska, Z., Volz, T., et al. (2014). Specific and nonhepatotoxic degradation of nuclear hepatitis B virus cccDNA. Science *343*, 1221–1228.

37. Zhou, L., Ren, J.H., Cheng, S.T., Xu, H.M., Chen, W.X., Chen, D.P., Wong, V.K.W., Law, B.Y.K., Liu, Y., Cai, X.F., et al. (2019). A functional variant in ubiquitin conjugating enzyme E2 L3 contributes to hepatitis B virus infection and maintains covalently closed circular DNA stability by inducing degradation of apolipoprotein B mRNA editing enzyme catalytic subunit 3A. Hepatology *69*, 1885–1902.

38. Landry, S., Narvaiza, I., Linfesty, D.C., and Weitzman, M.D. (2011). APOBEC3A can activate the DNA damage response and cause cell-cycle arrest. EMBO Rep. *12*, 444–450.

39. Vural, S., Simon, R., and Krushkal, J. (2018). Correlation of gene expression and associated mutation profiles of APOBEC3A, APOBEC3B, REV1, UNG, and FHIT with chemosensitivity of cancer cell lines to drug treatment. Hum. Genomics *12*, 20.

40. Green, A.M., Budagyan, K., Hayer, K.E., Reed, M.A., Savani, M.R., Wertheim, G.B., and Weitzman, M.D. (2017). Cytosine deaminase APOBEC3A sensitizes leukemia cells to inhibition of the DNA replication checkpoint. Cancer Res. *77*, 4579–4588.

41. Xu, C., Guo, Y., Liu, H., Chen, G., Yan, Y., and Liu, T. (2018). TUG1 confers cisplatin resistance in esophageal squamous cell carcinoma by epigenetically suppressing PDCD4 expression via EZH2. Cell Biosci. *8*, 61.

42. Li, X., Wu, Y., Liu, A., and Tang, X. (2016). Long non-coding RNA UCA1 enhances tamoxifen resistance in breast cancer cells through a miR-18a-HIF1α feedback regulatory loop. Tumour Biol. *37*, 14733–14743.

43. Li, L.J., Chai, Y., Guo, X.J., Chu, S.L., and Zhang, L.S. (2017). The effects of the long non-coding RNA MALAT-1 regulated autophagy-related signaling pathway on chemotherapy resistance in diffuse large B-cell lymphoma. Biomed. Pharmacother. *89*, 939–948.

44. Peng, W., Wu, J., and Feng, J. (2016). Long noncoding RNA HULC predicts poor clinical outcome and represents pro-oncogenic activity in diffuse large B-cell lymphoma. Biomed. Pharmacother. *79*, 188–193.

45. Peng, W., Fan, H., Wu, G., Wu, J., and Feng, J. (2016). Upregulation of long noncoding RNA PEG10 associates with poor prognosis in diffuse large B cell lymphoma with facilitating tumorigenicity. Clin. Exp. Med. *16*, 177–182.

46. Pandey, G.K., Mitra, S., Subhash, S., Hertwig, F., Kanduri, M., Mishra, K., Fransson, S., Ganeshram, A., Mondal, T., Bandaru, S., et al. (2014). The risk-associated long noncoding RNA NBAT-1 controls neuroblastoma progression by regulating cell proliferation and neuronal differentiation. Cancer Cell *26*, 722–737.

47. Yang, C., Wang, G., Yang, J., and Wang, L. (2017). Long noncoding RNA NBAT1 negatively modulates growth and metastasis of osteosarcoma cells through suppression of miR-21. Am. J. Cancer Res. *7*, 2009–2019.

48. Wei, L., Ling, M., Yang, S., Xie, Y., Liu, C., and Yi, W. (2021). Long noncoding RNA NBAT1 suppresses hepatocellular carcinoma progression via competitively associating with IGF2BP1 and decreasing c-Myc expression. Hum. Cell *34*, 539–549.

49. Guo, X., Xu, Y., Wang, Z., Wu, Y., Chen, J., Wang, G., Lu, C., Jia, W., Xi, J., Zhu, S., et al. (2018). A Linc1405/eomes complex promotes cardiac mesoderm specification and cardiogenesis. Cell Stem Cell *22*, 893–908.e896.

50. Liberzon, A., Birger, C., Thorvaldsdóttir, H., Ghandi, M., Mesirov, J.P., and Tamayo, P. (2015). The Molecular Signatures Database (MSigDB) hallmark gene set collection. Cell Syst. *1*, 417–425.

51. Rijal, S., Fleming, S., Cummings, N., Rynkiewicz, N.K., Ooms, L.M., Nguyen, N.Y., Teh, T.C., Avery, S., McManus, J.F., Papenfuss, A.T., et al. (2015). Inositol polyphosphate 4-phosphatase II (INPP4B) is associated with chemoresistance and poor outcome in AML. Blood *125*, 2815–2824.